PHYSICAL REVIEW B VOLUME 11, NUMBER 12 15 JUNE 1975

Electron tunneling into amorphous germanium*†

J. W. Osmun‡

Department of Physics, The University of Chicago, Chicago, Illinois 60637

(Received 17 June 1974)

A detailed study was undertaken of electron tunneling into amorphous Ge. At low temperature, $T \lesssim 100$ K, the high-field conductivity of the a-Ge film is similar to the tunneling conductance. For a-Ge thicknesses $t \lesssim 500$ Å the conductance of a-Ge blends smoothly with the tunneling conductance. This makes separation of tunneling conductance from the bulk a-Ge conductance difficult at low temperatures for junctions with thick a-Ge layers. The relation $\sigma = \sigma_0 \exp[-(T_1/T)^{1/4}]$ holds well for these junctions at zero bias for temperatures not showing bulk a-Ge effects. In junctions with sufficiently thin a-Ge layers, $t \approx 100$ Å, the bulk a-Ge does not seriously modify the conductance away from zero bias. A series of junctions formed on the same oxide with $t \leq 80$ Å of a-Ge show an exponential drop in conductance with increasing t leveling off at temperature-dependent values. This is interpreted as incomplete surface coverage. This interpretation is independent of the details of the tunneling mechanism into a-Ge, but does place an upper limit on the possible tunneling range, varying from 28 Å at 300 K to 50 Å at 4.2 K. Tunneling thus only probes the surface layers of a-Ge and does not reflect the bulk properties. Capacitance studies of the junctions indicate the presence of a high density of interface states, $N_s \geq 2.5 \times 10^{14}$ eV^{-1} cm^{-2}. Superconductive tunneling confirms that tunneling is the dominant conduction mode for these junctions.

I. INTRODUCTION

Electron tunneling through a thin oxide into an amorphous semiconductor has been the subject of several investigations[1–5] with the anticipation of obtaining information about the density of states within the band gap of the semiconductor. Since initial and final tunnel states are not both Bloch states a cancellation[6] of density of states in the tunneling conductance is not expected. If it can be shown that the tunneling data do in some way show density of states, the validity of various models for the distribution of states in the band gap could be tested.

Most amorphous semiconductors so far investigated by means of tunneling, including Ge,[1–3] Si,[2–4] InSb,[3,5] and GaSb,[5] have tetrahedral short-range order. All these materials exhibit quite similar tunneling conductance-voltage (G-V) characteristics. The conductance rises smoothly and symmetrically about a minimum exactly at zero bias, increasing several orders in magnitude as the applied bias is increased to ±1 V. As the temperature is decreased the lower-bias conductance decreases in magnitude more rapidly than the conductance at higher biases, resulting in a deeper and sharper conductance minimum at lower temperatures. At first glance these curves appear remarkably similar to what one might expect from a direct application of the Mott-CFO (Cohen, Fritzsche, Ovshinsky)[7,8] model for amorphous semiconductors.

The Mott-CFO model has as its main features (i) conduction and valence band states tailing deep into the band gap and (ii) mobility edges E_c and E_v marking the transition in energy from localized to extended states. The model predicts low tunneling probability or conductance when tunneling occurs from or into states near the center of the gap due to a low density of localized midgap states. As the bias is increased tunneling into higher density of states closer to the mobility edges gives rise to a rapidly increasing conductance. Smith and Clark[2] have extracted a density of states by a direct comparison of metal-oxide–semiconductor–metal (MOSM) and metal-oxide–metal (MOM) data for junctions using amorphous Ge and Si, obtaining for the density of states

$$N(eV) = G_{MOSM}/G_{MOM} , \qquad (1)$$

where G_{MOSM} and G_{MOM} are conductances for the MOSM and MOM junctions, respectively. One of the most obvious defects of this direct approach is its failure to account for the temperature dependence of the tunneling characteristics.

In order to explain the temperature dependence of tunneling conductance Sauvage, Mogab, and Adler[9] have proposed a variable-range tunneling model using arguments quite similar to those in Mott's[10] derivation of the $\ln\sigma$ vs $T^{-1/4}$ law for hopping conduction in amorphous semiconductors. They pointed out that an electron tunneling through the oxide must tunnel an additional distance into the semiconductor to find a localized state. This distance is determined by the average spatial separation of states within dE of E at T. Phonon assistance allows an electron to tunnel into states of different energies located closer to the barrier. As the temperature is lowered fewer phonons are available and an electron must tunnel further to find a final state. This yields a tunneling probability

$$P \propto e^{-2\alpha_0 d_0} e^{-(T_1/T)^{1/4}} , \tag{2}$$

where

$$T_1 = 36\alpha_s^3 / N(E)K \tag{3}$$

α_0 and d_0 are the wave-function decay constant and the thickness of the oxide, respectively, and α_s is the wave-function decay constant of the semiconductor. Their experimental data on a-Si (a means amorphous) do indeed show a $\ln G \propto T^{-1/4}$ behavior over the measured temperature range of 78–300 K. From the slope of the temperature dependence they extract a density of states for a-Si at the Fermi level of approximately 5×10^{19}/eV cm^3, rising rapidly with increasing energy separation from this minimum.

Because the conductance minimum appears at zero bias any density-of-states interpretation of the data leads unavoidably to the conclusion that the Fermi level in the semiconductor lies at the density-of-states minimum. This is unlikely to occur in different materials prepared in various laboratories under differing preparation conditions. While having the conductance minimum appear at zero bias seems to be characteristic of tunneling into amorphous tetrahedral semiconductors, this is not necessarily true of amorphous semiconductors in general. Tunneling data[11] on an amorphous chalcogenide alloy, $Tl_2SeAs_2Te_3$, of relatively high conductivity, show a conductance minimum at $V = 0.070$ V with respect to the metal electrode.

An objection to the apparent agreement between the tunneling data in a density-of-states interpretation and the Mott-CFO model is that the model was not expected to apply to simple tetrahedrally coordinated amorphous semiconductors. A more structured density of states is expected for these materials, such as that obtained by Spear and Le Comber[12] from field-effect measurements on plasma-decomposed SiH_4. An alternative suggestion has been to look at the tunneling data as a surface-state phenomenon.[1]

The purpose of this investigation is to look in greater detail at one system, involving a-Ge, to see if further useful information can be obtained. We will look at the nature of the bulk a-Ge effects on the conductance data, extend the range of the temperature dependence down to 4.2 K, investigate the range of tunneling into the semiconductor, use superconductive tunneling as a test, and look at the capacitance of the junctions. High magnetic field dependence is also considered.

A preliminary report of portions of this investigation has already been given.[13]

II. EXPERIMENTAL PROCEDURE

The tunnel junctions used in this study were fabricated in an oil diffusion pumped system with a liquid-nitrogen trap. The substrates for the junctions were of optically flat Pyrex thoroughly cleaned and with a final rinse of reagent-grade ethanol before installation in the vacuum system. The first evaporation consisted of approximately 2000-Å Al, 99.999% pure, to form the bottom electrode. Next the Al was oxidized in an oxygen plasma at 0.1 Torr for approximately 60 sec, the time varying to obtain different junction impedances. After pumping back down to 2×10^{-7} Torr, Ge was evaporated, obtaining the required thickness by using a rotating shutter in a constant evaporation flux. Different Ge thicknesses could be obtained for each of six junctions on a substrate. This was followed by evaporating on top of the a-Ge a counterelectrode of 1500-Å Al in order to reduce the current path in the a-Ge and thus the undesired resistance in series with the junction. An alternative counterelectrode material was pure Sn. Finally a thin layer of SiO was deposited for junction protection. No edge protection was provided. The entire procedure was completed before exposure to atmosphere. Junction areas were approximately 6×10^{-3} cm^2. Film thickness was monitored using a quartz-crystal microbalance. The substrate remained at room temperature during fabrication.

Tunneling characteristics were obtained by hand differentiation of current-voltage (I-V) curves. Electronic differentiation proved impractical due to large changes in junction impedance with bias and due to long time constants arising from junction capacitance. I-V curves were obtained by four-terminal measurements using a Keithley 604 differential electrometer amplifier for measuring voltage and a Keithley 610C electrometer for current. When measuring the low voltages in superconductive tunneling a Keithley 153 microvolt-ammeter was used for voltage at the sacrifice of input impedance.

The samples were measured in a helium cryostat with temperature adjustment obtained by use of helium exchange gas. The lowest temperatures were obtained by direct immersion in liquid He. The temperature was monitored using a copper-constantan thermocouple or a carbon resistance thermometer, depending on the temperature range. For superconductive tunneling measurements the temperature was obtained from a fit of the BCS theory to the superconducting energy gap of Al.

The junctions were mounted in the cryostat and cooled down as soon as possible after fabrication. This was done to retard annealing effects, which will be discussed in a subsequent section.

III. a-Ge CONDUCTIVITY AND TUNNELING CHARACTERISTICS

Before proceeding with an investigation of the low-temperature conductance of tunnel junctions

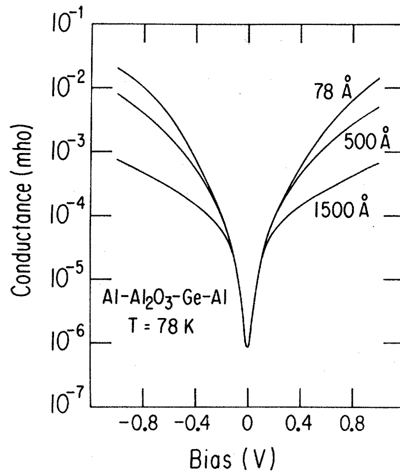

FIG. 1. Conductance as a function of voltage for Al-Al_2O_3-Ge-Al junctions with 78-, 500-, and 1500-Å a-Ge at 78 K. The first two curves are normalized to the value of G for 1500-Å a-Ge at zero bias, shifting $\lesssim 20\%$.

involving an amorphous semiconductor it is necessary to understand how the bulk resistance of the semiconductor affects the measured total conductance. In a MOSM tunnel junction the current flowing through the junction also flows through the semiconductor layer. This layer adds a series resistance to the tunneling resistance and the applied voltage is divided between the junction and the semiconductor layer. If the tunneling resistance increases more slowly than the bulk resistance of the semiconductor, eventually a temperature is reached at which the tunneling conductance is noticably modified by the a-Ge conductance. This is demonstrated in Fig. 1, where we show G-V characteristics for three different a-Ge thicknesses

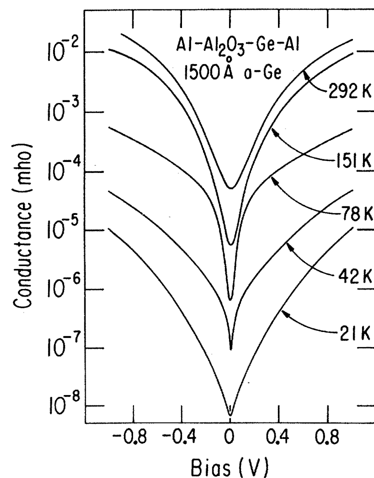

FIG. 2. Conductance as a function of voltage for a tunnel junction with 1500-Å a-Ge at several temperatures.

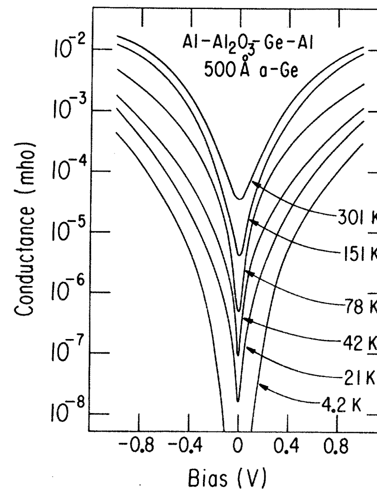

FIG. 3. Conductance as a function of voltage for a tunnel junction with 500-Å a-Ge at several temperatures.

measured at 78 K. For clarity the curves have been shifted ($\lesssim 20\%$) to have the same magnitude at zero bias. These curves overlap each other at low biases, indicating that G is dominated there by the oxide and oxide-semiconductor interface regions, not by the bulk a-Ge. As the a-Ge thickness is increased the effect of the a-Ge series resistance becomes increasingly dominant at higher biases, resulting in a slower rise of the curve for 1500 Å. It is clear here that the first sign of a series resistance is this decrease in the slope of the G-V curve at high biases. The zero-bias conductance of a MOM junction, formed on the same substrate as the MOSM junction with 78-Å a-Ge, was 10^{-1} mho. Such oxides in MOM junctions tended to break down easily at high biases, so measurements were restricted to low biases. MOM junctions with thicker oxides have the same parabolic characteristics commonly found for tunnel junctions.[14]

Figures 2 and 3 show the G-V characteristics for tunnel junctions with 1500 and 500 Å of a-Ge, respectively. Both junctions were formed on the same oxide layer so that they are identical in all other respects. The curves remain approximately symmetric about a minimum at zero bias for all temperatures. The 1500-Å film in Fig. 2 shows the decrease in slope of the G-V curve at high biases quite clearly at and below 78 K, indicating the presence of the series resistance. As the temperature is reduced from 78 K the bias voltage at which the decrease in slope becomes apparent is also reduced, until at 21 K the a-Ge film dominates the conductance at all biases. However, as the temperature is reduced below 78 K the decrease in slope, which indicated the presence of the a-Ge film resistance, becomes increasingly less pronounced. For the 500-Å film in Fig. 3 the changes

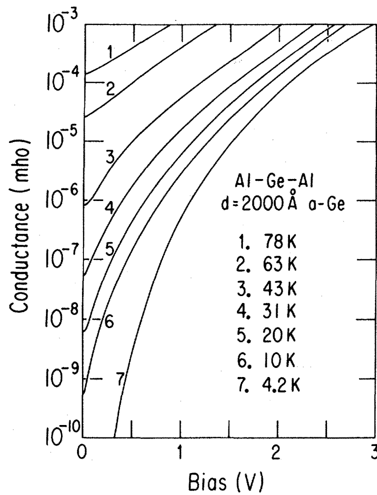

FIG. 4. High-field conductance as a function of voltage for 2000-Å a-Ge in Al-Ge-Al sandwich configuration for several temperatures.

in slope of the G-V curves at higher biases, while present, are not as noticable. Again, the decrease in slope first observed at 78 K becomes increasingly less pronounced as the temperature is further lowered. The similarities and differences in Figs. 2 and 3 can be understood by considering the high-field conductivity of a-Ge films.[15,16]

The behavior of high field conductivity is demonstrated by the conductance-voltage characteristics for an Al–a-Ge–Al sandwich containing 2000-Å a-Ge, shown in Fig. 4. The sample was prepared following the same procedure as for a tunnel junction, but omitting the oxidation step. The G-V characteristics are presented for several temperatures from 78 down to 4.2 K. At higher temperatures current heating gave unreliable high-field data. An applied potential of 1 V across a 2000-Å film yields an average field of 5×10^4 V/cm. As the temperature is reduced the field dependence of the conductivity rapidly increases. At 4.2 K a change of field from 1.5×10^4 V/cm to 1.5×10^5 V/cm corresponds to a change in conductance of 10^7. At low temperatures the voltage dependence of the bulk a-Ge conductance and this voltage dependence of total tunnel junction conductance look very similar.

It is now possible to extract quantitatively the true junction conductance from the measured G-V curves. Since the voltage is divided between the oxide layer and the a-Ge film, the system can be approximated as two voltage-dependent resistors in series, yielding two relationships for the tunnel conductance:

$$V(I)=V_1(I)-V_2(I) \tag{4}$$

and

$$\frac{1}{G(V)}=\frac{1}{G_1(V_1)}-\frac{1}{G_2(V_2)}\ , \tag{5}$$

where the current is the same through both resistors and subscripts 1 and 2 refer to measured MOSM and MSM parameters, respectively. Contact resistance at the metal-semiconductor interface has been neglected since no known experiments have shown its existence for a-Ge. Figure 5 shows G-V curves for the junction with 1500-Å a-Ge, now corrected for the presence of the a-Ge. Under the assumption that the applied field scales with thickness, V_2 and G_2 were scaled by a thickness factor 1.33. The curve at 292 K needed no correction, and the correction to the 151-K data used only the ohmic, low-field resistance of the a-Ge. For the curve at 42 K at an applied bias of 1 V, 0.74 V drops across the a-Ge layer, bringing the corrections well into the high-field region. Figure 5 and other corrected data representing the true junction conductance will be discussed in the next section.

As the thickness of the a-Ge layer is decreased the separation of the behavior into two distinct voltage-dependent resistances no longer remains a valid approximation. The a-Ge layer constitutes one side of the junction, so that the approximation is valid only when the a-Ge thickness is much greater than the average tunneling distance into the Ge. Also, we have not established whether the high-field behavior of a-Ge scales with thickness. The question of whether the conduction at high fields in thin films of a-Ge is contact or bulk limited has not yet been settled. In addition, fluctuations in film thickness become increasingly important for thin films at high fields and low temperatures. Because of these uncertainties the correction of the

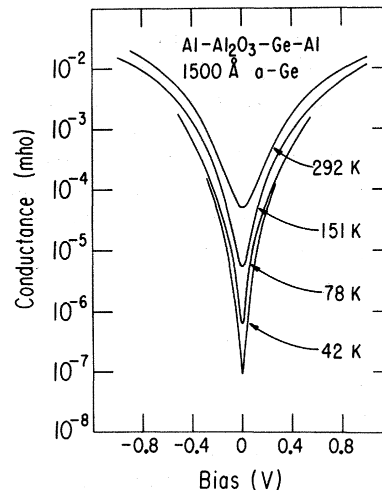

FIG. 5. Conductance as a function of voltage for a tunnel junction with 1500-Å a-Ge corrected for the presence of the a-Ge series resistance.

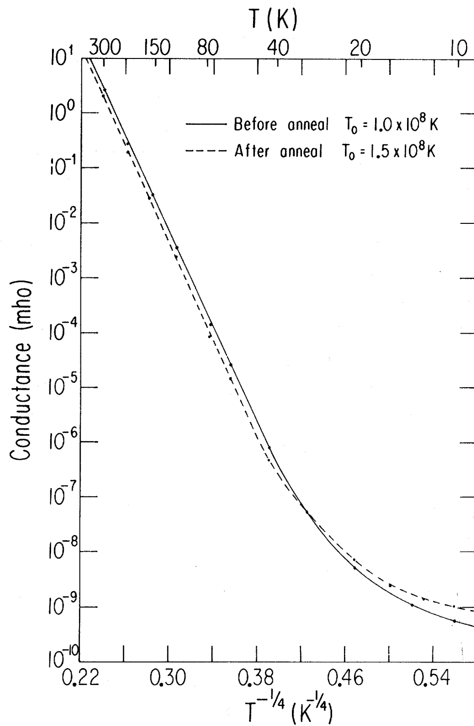

FIG. 6. Temperature dependence of zero-bias conductance for 2000-Å a-Ge. Dashed curve is for sample after annealing 1 month at 300 K.

junction containing 500-Å a-Ge was not as successful as that obtained for thicker a-Ge, especially away from zero bias. Clearly a more detailed model of the device behavior is needed for this range of a-Ge thicknesses. For junctions with thin a-Ge films the tunneling conductance blends in smoothly with the high-field conductivity, making it difficult to tell visually when the a-Ge becomes important.

A detailed consideration of the ohmic behavior of the a-Ge conductivity is desirable because of the similarity of the variable-range tunneling model[9] to Mott's hopping model[10] for conduction in a-Ge near the Fermi energy E_F. Mott's model describes conduction near E_F by thermally assisted tunneling to spatially available states of the proper energy, obtaining for the conductivity

$$\sigma(T) = \sigma_0 e^{-(T_0/T)^{1/4}} \quad , \tag{6}$$

where T_0 as derived by Ambegaokar, Halperin, and Langer[17] is

$$T_0 = 16\alpha^3/N(E_F)k \quad . \tag{7}$$

α, k, and $N(E_F)$ are, respectively, the wave-function decay constant, the Boltzman constant, and the density of states at E_F. In Figure 6 the logarithm of the ohmic conductivity for the 2000-Å a-Ge film is plotted as a function of $T^{-1/4}$. A straight line is obtained from 300 K down to approximately 40 K. Below 40 K the curve deviates sharply from the predicted behavior. The slope of the straight line in Fig. 6 gives 1.0×10^8 K as the value for T_0. Using Eq. (6) and assuming a reasonable value for α of 10^7 cm^{-1}, we obtain $N(E_F) = 1.9\times10^{18}$ eV^{-1} cm^{-3} for the density of states at the Fermi level. This value for T_0 is within the range of what other investigations have found for a-Ge.[16,18]

The deviation of the conductivity from the $T^{-1/4}$ behavior is surprising and was not anticipated. Figure 4 shows that at low temperatures the high-field effects are quite strong at fields of less than 10^3 V/cm. Transient effects with long time constants at low temperatures and low fields were observed, such as reported by Morgan and Walley[16] in their study of the conductivity of a-Ge. These time constants were particularly noticable immediately after high-field measurements. This suggested that the time constants and possibly the deviation from Eq. (6) arose from a frozen-in disequilibration of the electron distribution by the high field previously applied. To check this the sample was remeasured after storage at room temperature for one month. The maximum field applied until completion of the low-field measurements was 5×10^2 V/cm, still within the ohmic range for all measured temperatures. The results of these measurements are shown by the dashed line in Fig. 6. The deviation from the $\ln\sigma$ vs $T^{-1/4}$ behavior is still present, but the long time constants were not observed. As a result of aging for one month at room temperature the conductivity at higher temperatures became lower while still following the $T^{-1/4}$ law. The slope became greater, having $T_0 = 1.5\times10^8$ K. This is consistent with an interpretation of annealing out of defect states and dangling bonds within the a-Ge. The low-temperature deviation from Eq. (6) now appears to begin at a slightly higher temperatures than before. At the lowest temperatures the sample is now less resistive than before aging.

The low-temperature deviation from Eq. (6) can be interpreted as a consequence of long-range potential fluctuations[19] arising from heterogeneities, screened Coulomb potentials, and voids. At low temperatures the rather high internal fields cause modification of the variable-range hopping in such a way that higher conductivity than predicted by Eqs. (6) and (7) arises. Alternatively, the deviation may arise from impurities introduced during evaporation.

The effect of aging on the conductivity of a-Ge above 40 K, seen in Fig. 6, is similar to heat treatment above room temperature—the result is an increase in resistance. A freshly formed a-Ge film is not at equilibrium at room temperature until it has been aged for many days or annealed

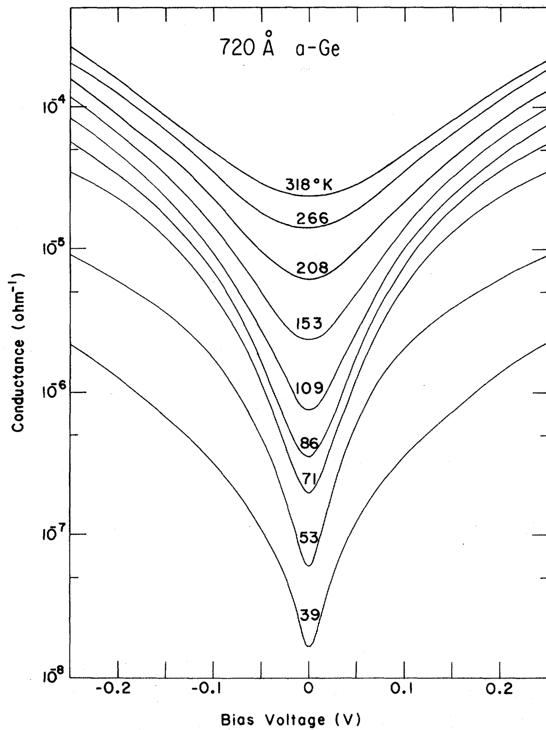

FIG. 7. Conductance as a function of voltage for a tunnel junction with 720-Å a-Ge at several temperatures.

at a higher temperature. The high-field conductivity, after being normalized to the value at zero bias, shows no noticable difference at 78 K as a result of aging. Similarly, tunnel junctions show an increase in resistance as a result of aging or heat treatment. After normalizing the conductances at zero bias there is little difference in the G-V characteristics. This is not surprising because it is well known that oxides continue changing after fabrication, resulting in a scaling of the tunneling current. For a tunnel junction this could result in a factor of 10 change in conductance. It was to avoid this that samples were cooled to low temperatures soon after fabrication. No systematic investigation was made of the effects of aging and heat treatment.

IV. TUNNELING INTO a-Ge

The temperature dependence of tunnel conductance can be profitably investigated by measuring junctions at temperatures safe from any bulk a-Ge effects. The low-bias G-V characteristics for a junction containing 720-Å a-Ge are shown in Fig. 7 for several temperatures. The effect of the a-Ge series resistance is apparent above $V = 50$ mV, but the zero-bias conductance is still not noticably affected even at 39 K. The data for this junction is plotted in Fig. 8 with log G as a function of $T^{-1/4}$ for $V = 0$, -100 mV, and -250 mV. As predicted by Eq. (2) a good fit to a straight line is obtained at zero bias for the entire measured range, down to 31 K. Conductances at higher biases show a tendency toward becoming independent of temperature at low T, but the series resistance of the a-Ge takes over and conductance falls rapidly. The straight line at zero bias yields $T_1 = 3.9 \times 10^6$ K. This is within the range of values for T_1 found by Hauser[3] in his investigation of tunnel junctions with sputtered a-Ge. Using Eq. (3) this gives a density of states at the Fermi level of $N(E_F) = 1.1 \times 10^{20}$ eV^{-1} cm^{-3}, assuming $\alpha_s = 10^7$ cm^{-1}.

We now return to the true junction conductance as obtained from the data of the junction with 1500-Å a-Ge after correcting for the series resistance of the semiconductor. Figure 5 shows that the conductance has little temperature dependence at high biases, but is quite temperature dependent at low biases. The data for this junction is plotted as a function of $T^{-1/4}$ in Fig. 9 for several biases. Data corrected for the a-Ge resistance is represented by an x. The zero-bias conductance follows the $T^{-1/4}$ behavior of Eq. (2) down to $T \simeq 50$ K. The straight line gives a slope of $T_1 = 3 \times 10^6$ K. Below approximately 50 K the data deviate from the $T^{-1/4}$ behavior. At higher biases the conductance becomes temperature independent.

The alternative to applying corrections to the data is to attempt to obtain junctions in which the a-Ge layer is sufficiently thin as to make a correction unnecessary. The main problem that arises here is the possible presence of pinhole shorts. While tunnel junctions with thin layers of a-Ge are easily fabricated to give reproducible data above 78 K, this is not true for the same junctions at lower temperatures where the conductances are low. There

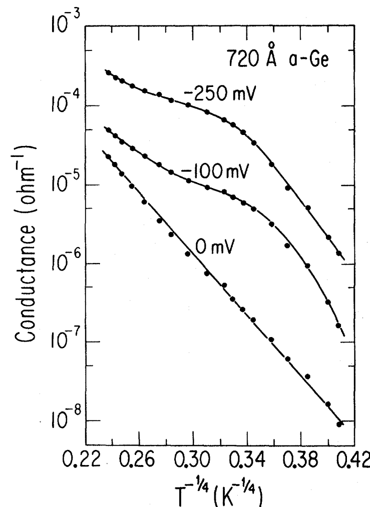

FIG. 8. Conductance as a function of $T^{-1/4}$ for a tunnel junction with 720-Å a-Ge at zero bias, -100 mV, and -250 mV.

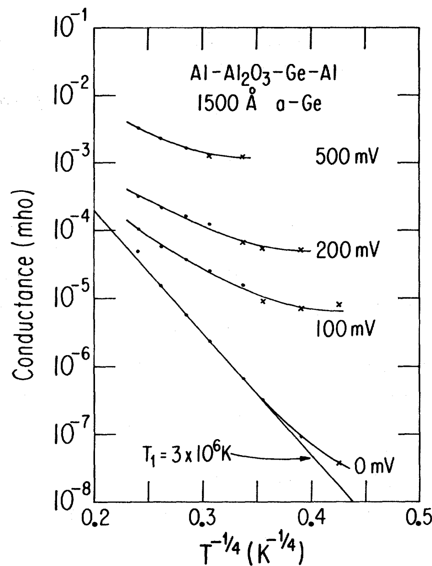

FIG. 9. Conductance as a function of $T^{-1/4}$ for a junction with 1500-Å a-Ge at several biases, corrected for the a-Ge series resistance.

are two possible origins for higher-conductance leakage paths. The first is that as the film starts to grow the atoms migrate on the surface and form clusters. The space between clusters allow for shorting paths when the counterelectrode is deposited. The presence of such shorts becomes apparent when the a-Ge thickness $d \lesssim 50$ Å. A second source of leakage paths is important for junctions with up to several-hundred-Å a-Ge. They may possibly arise from microscopic particles of foreign matter on the oxide surface. Since the junctions become very resistive at low temperatures the surface must be free of such particles to better

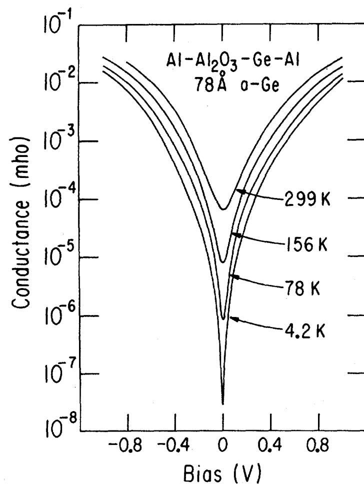

FIG. 10. Conductance as a function of voltage for a tunnel junction with 78-Å a-Ge at several temperatures.

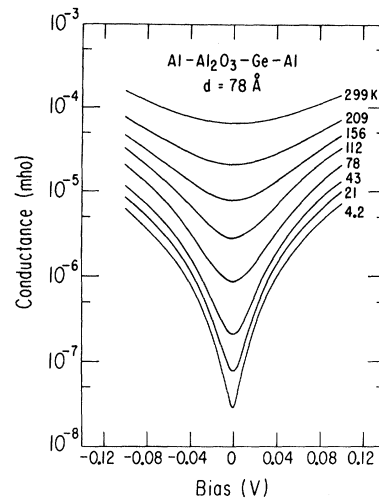

FIG. 11. Low-bias conductance as a function of voltage for a tunnel junction with 78-Å a-Ge at several temperatures.

than 1 part in 10^7. The a-Ge and the shorts form parallel current paths for the tunneling electrons. Since MOM junctions have temperature-independent conductances, the presence of shorts results in a limiting minimum conductance for the entire junction. As the temperature is lowered the conductance reaches this limiting value and the conductance starts to broaden at the minimum. With this understanding of the behavior of shorts, we have used the sharpness of the G-V characteristics at low temperatures as a measure of the quality of the tunnel junction.

A junction showing little evidence of shorts is presented in Fig. 10, where the G-V characteristics at several temperatures are shown for a MOSM junction containing 78-Å a-Ge. These curves are strikingly similar to those of Fig. 5. There is very little temperature dependence for the conductance at high biases. At low biases the temperature dependence is strong, giving sharp G-V curves at the lowest temperatures. More detailed data for the low-bias region of the junction is given in Fig. 11. The sharpening is quite pronounced. At 1.2 K the curve is identical to that at 4.2 K, indicating that thermal broadening is not yet an important factor. There is a slight asymmetry to the curves at the lowest and highest temperatures. These asymmetries may be seen in Figs. 10 and 11 by comparing the conductance at positive and negative biases of equal magnitude near the higher-bias regions of the curves. They are slight in that the conductance differs by no more than a factor of 2 for opposite biases. The high-temperature asymmetry is the same as that of a MOM junction and is caused by the shape of the oxide barrier potential.[14] The low-temperature asymmetry has the

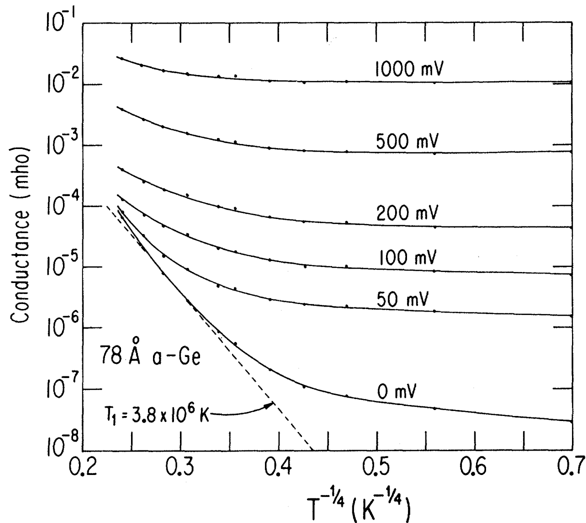

FIG. 12. Conductance as a function of $T^{-1/4}$ for a tunnel junction with 78-Å a-Ge at several biases. Dashed line is straight line at higher temperatures after correction for slight temperature dependence of MOM conductance.

opposite sign. At high biases, as shown in Fig. 10, the G-V curves have the same asymmetry, attributable to the oxide. The cross-over in sign of the low-bias asymmetry occurs at approximately 80 K. The asymmetry at 4.2 K indicates that the conductance minimum may occur at −1 mV, but this is within the broadening of the curve. Log$G$ vs $T^{-1/4}$ is plotted in Fig. 12 for these data at various biases. The oxide for this sample was found to give a slightly temperature-dependent conductance at high temperature when in a MOM junction, becoming temperature independent below 200 K. If the zero-bias data are corrected for this temperature dependence, the high-temperature data can be fitted with a straight line, according to Eq. (2). This line gives a slope of $T_1 = 3.8 \times 10^6$ K. Below 100 K there is a marked deviation from $T^{-1/4}$ behavior. At biases above 50 mV there is very little temperature dependence below 30 K.

The similarity of the corrected G-V curves in Fig. 5 with the data shown in Fig. 10 for a junction with 78-Å a-Ge is not surprising. Corrections to the conductance due to the a-Ge for junctions with very thin a-Ge layers are not expected to be very important away from zero bias. With 78 Å the a-Ge is thin enough for the conductivity to be well into the high-field region when only small fraction of the applied voltage drops across the semiconductor. In contrast to the behavior of junctions with a thick a-Ge layer, corrections to the conductance are now of most importance near zero bias. Evidence for the effect of the a-Ge resistance in junctions with thin a-Ge layers is given in Fig. 13. The G-V characteristics at 4.2 K are shown for two junctions formed on the same oxide, one with 78-Å a-Ge and the other with 52-Å a-Ge. Only positive bias is shown. The junction with 78-Å a-Ge has a noticably broader G-V curve. This difference between these curves can be attributed solely to the differences in a-Ge thickness. In these junctions the transition from tunneling-dominated conductivity to a-Ge-dominated conductivity is so smooth that an exact description of the tunneling and conductivity mechanisms is needed to separate the two. Furthermore, it is not possible to make the a-Ge thin enough to ignore its contribution as a series resistance at low temperatures.

A comparison of Fig. 6 with Figs. 9 and 12 indicates that the deviation from the $T^{-1/4}$ behavior at zero bias for the tunnel junctions is similar to the deviation for the a-Ge film. This suggests that the MOSM conductance at low biases and low temperatures is related to the a-Ge conductance. Small nontunneling leakage currents through the oxide, which would be noticable only at low conductance, could cause this. If this is so the low-temperature asymmetry previously noted can be explained as arising from a slightly asymmetric conductance for the a-Ge, which in turn results from having an O-S interface on one side and an S-M interface on the other. Comparison of Figs. 8 and 12 reveals a major discrepancy in the temperature dependence of conductivity at zero bias for the two junctions. The tunnel junction containing 720-Å a-Ge obeys the $T^{-1/4}$ law down to at least 31 K, while the junction with 78-Å a-Ge deviates from the $T^{-1/4}$ behavior below 100 K. This indicates that it may take a fairly thick a-Ge film to properly establish the low-temperature conductance.

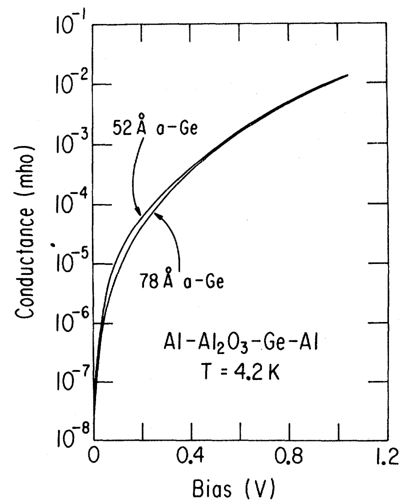

FIG. 13. Conductance as a function of voltage at 4.2 K for two tunnel junctions formed on the same oxide, one with 78-Å a-Ge and one with 52-Å a-Ge.

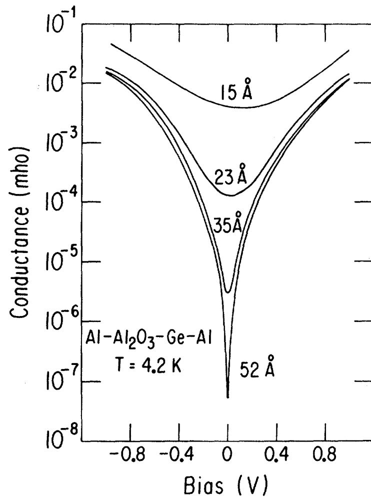

FIG. 14. Conductance as a function of bias voltage at 4.2 K for Al-Al_2O_3-Ge-Al tunnel junctions with several thicknesses of a-Ge.

An attempt was made to determine if the bias dependence of the conductance is modified by a high magnetic field. The MOSM tunnel junction with 78-Å a-Ge was measured at 4.2 K in a field of 65 kG. No change in conductance was observed to within 1%.

V. PARTIAL SURFACE COVERAGE

In the last section it was noted that for junctions with sufficiently thin a-Ge layers the total conductance away from zero bias is not seriously modified by the a-Ge conductance. However, minor differences between G-V curves with 52-Å a-Ge and 78-Å a-Ge were attributed to the difference in a-Ge thickness. This means that the electrons tunnel to and from states in the a-Ge less than 78 Å from the oxide, and possibly less than 52 Å. In order to obtain information about what happens near the junction interface and possibly learn how far an electron tunnels into the a-Ge an examination was undertaken of junctions with very thin a-Ge layers.

Samples were prepared with six junctions on the same oxide. One junction of the six contained no a-Ge, forming a MOM junction, while the remainder had increasing thicknesses of a-Ge. The G-V characteristics for a set of these junctions measured at 4.2 K are shown in Fig. 14. The zero-bias conductance of the MOM junction is 1.0×10^{-1} mho. The last junction, containing 78-Å a-Ge, is not included on this figure, for as already shown the conductance change is not substantial as the a-Ge thickness is increased to 78 Å. There is little change in conductance with a-Ge thickness at high biases, but the zero-bias conductance changes rapidly. The minimum for the curves with 15- and 23-Å a-Ge is not at zero bias. This offset of the minimum is similar to the behavior of a MOM junction, for which the minimum is offset by the asymmetry of the oxide barrier potential. For these two junctions the fraction of the total junction area not covered by a-Ge is sufficient to be seen clearly in the G-V characteristics.

The zero-bias conductance as a function of a-Ge thickness is plotted in Fig. 15 for several temperatures, with the MOM junction being represented by thickness $t=0$. The curves are drawn to connect the six points for each temperature. The a-Ge thicknesses, 15, 23, 35, and 78 Å, represent the average thickness values as determined by the quartz-crystal microbalance assuming homogeneous layers and a density of 5.32 g/cm^3 equal to that of crystalline Ge. Since the true density of the a-Ge film is known to be less, the thickness may be larger by as much as (10–15)%. The counterelectrode for these junctions is Al. Figure 15 shows that the conductance rapidly decreases with increasing Ge thickness, becoming thickness independent at different thicknesses as the temperature is changed. At 300 K the change in conductance levels off at $t\simeq 28$ Å and at 4.2 K the leveling off begins at $t\simeq 50$ Å. The zero-bias conductance as a function of a-Ge thickness for a similar set of junctions with Sn as the counterelectrode is shown in Fig. 16. The MOM conductance has an anomalously low value. When one deals with such small thicknesses the alloying and oxidation properties of the counterelectrode materials are expected to have an important effect. These effects become increasingly less important as the a-Ge thickness is increased. The point of interest here is that the behavior for thicker a-Ge films in Fig. 16 is similar to that in Fig. 15. Again, for the junctions with 15- and 23-Å a-Ge the minimum in conductance

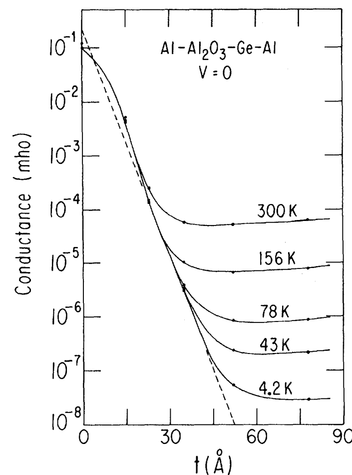

FIG. 15. Zero-bias conductance as a function of a-Ge thickness for Al-Al_2O_3-Ge-Al junctions with the same oxide.

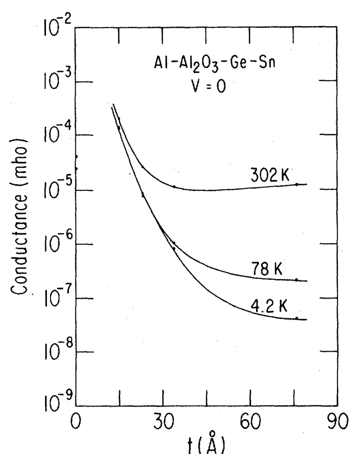

FIG. 16. Zero-bias conductance as a function of a-Ge thickness for Al-Al_2O_3-Ge-Sn junctions with the same oxide.

was not at zero bias, indicating that surface coverage was not complete and that the current near zero bias is flowing through MOM shorts in the MOSM junction.

The data in Figs. 13–15 can be interpreted in two alternative ways. The first interpretation assumes that the a-Ge surface coverage is uniform and that the exponential drop in tunneling conductance with increasing a-Ge thickness arises from direct tunneling from electrode to electrode, following the variable-range tunneling model.[9] This interpretation was discussed adequately in the preliminary report of the experiment,[13] so we now turn to the alternative interpretation, which considers the effects of leakage paths through the a-Ge layer.

We have already seen from Fig. 14 that the zero-bias conductance for junctions with 15- and 23-Å a-Ge is determined by incomplete surface coverage. The area of incompleted surface coverage in junctions with more a-Ge would not have a large enough fraction of the total surface area to move the conductance minimum away from zero bias, but would be able to limit the conductance minimum at low temperatures. At 4.2 K the conductance is so low for complete surface coverage that shorts with very small fractional areas are important. At higher temperatures where the conductance for complete coverage is greater it takes shorts with larger areas to be important. A simple model recently used by Gray[20] describes the fraction of the junction area not covered with a-Ge. Assume that atoms strike the surface randomly and remain where they strike. Divide the surface into N cells, each the size of a Ge atom. The probability of a vacant cell for n atoms striking the surface is

$$P=(1-1/N)^n \quad . \tag{8}$$

For large N this becomes

$$P(x)=e^{-x}=e^{-t/a} \quad , \tag{9}$$

where $x=n/N$ is the average number of monolayers, t is the film thickness, and a is the monolayer thickness. The dashed line in Fig. 15 describes the exponential drop in conductance with thicknesses for $20 \leq t \leq 45$ Å. This line is described quite well by Eq. (9) when $a = 3$ Å, a quite reasonable value.

The assumption of no surface mobility in this model is valid for a-Ge after the first few monolayers. In the first few monolayers the surface mobility is important in forming clusters and in concentrating the fraction of the junction surface not covered with a-Ge atoms into relatively large areas. Then an atom striking a Ge cluster on the surface during fabrication finds a bonding site anywhere it strikes. If an atom strikes a region without any Ge it can move about until it finds a site on the edge of a cluster. Thus an atom striking an unoccupied cell will eventually remain in a previously unoccupied cell while an atom striking an occupied cell will remain in an occupied cell. Surface mobility allows the unoccupied cells to remain connected but cancels out in describing the total fraction of the surface these unoccupied cells comprise. The fractional area is described, but not the size and distribution of the unoccupied areas. The model breaks down when the size of the unoccupied areas becomes too small to allow the counterelectrode to form a path through the a-Ge. The assumption of no surface mobility has been used by Henderson[21] to describe the growth of voids in a-Ge and a-Si. These voids have been seen by electron microscopy in several investigations.[22,23] The model discussed here considers these well known voids for the case of very thin films.

This interpretation of the tunneling data for very thin a-Ge layers offers no information about the tunneling mechanism and thus does not explain the temperature dependence of the tunneling conductivity. However, an important consequence is that it requires the electrons to tunnel to and from states in the semiconductor within a few monolayers from the oxide. It places an upper limit to the possible tunneling range into the semiconductor, varying from 28 Å at 300 K to 50 Å at 4.2 K.

Both the tunneling-range interpretation and the partial-surface-coverage interpretation have electrons tunneling directly from one metal electrode to the other to explain the data obtained on junctions with very thin a-Ge layers. They both explain the temperature independence of the zero-bias conductance at low temperatures as well as the decrease in conductance with increasing a-Ge layer thickness. Both interpretations give conductance of the correct order of magnitude using rea-

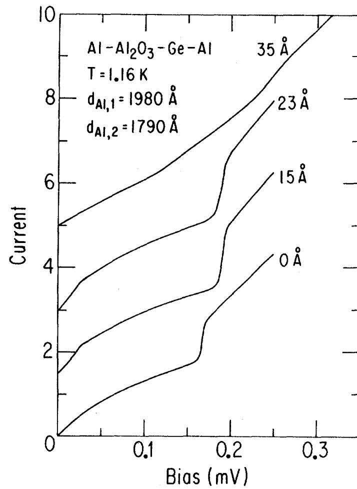

FIG. 17. Current as a function of voltage at 1.16 K for Al-Al_2O_3-Ge-Al tunnel junctions. The current scales per division for the different a-Ge thicknesses are (a) 0 Å: 5×10^{-6} A; (b) 15 Å: 1.67×10^{-7} A; (c) 23 Å: 5×10^{-9} A; and (d) 35 Å: 1.67×10^{-10} A. Current axis is offset for clarity.

sonable physical parameters. From available data it is not possible to determine which is correct. Since both interpretations are insensitive to changes in conductance of a factor of 2 it may be that both tunneling range and partial surface coverage are important in determining the tunnel conductance. In consideration of the known fluctuations in thin film thickness and the occurrence of voids in a-Ge we consider the incomplete-surface-coverage interpretation to be more reasonable.

VI. SUPERCONDUCTIVE TUNNELING

Both the hypotheses mentioned in the last section, the incomplete surface coverage and tunneling range, require that the dominant conduction mechanism for thin a-Ge films be direct tunneling from metal electrode to metal electrode. While not able to distinguish between these two hypotheses, the observation of the gap in the density of states as the metal electrodes become superconducting can determine whether the tunneling is direct or indirect involving several states. Superconductive tunneling can also tell us if tunneling is indeed the dominant conduction mechanism. Early confirmation of tunneling involved using oxides independently checked in MOM configurations or using plausibility arguments. Recently Hauser[3] observed the superconductive properties in Al-Al_2O_3-Ge-Pb junctions.

The set of junctions that were shown in Fig. 14, where the thickness of a-Ge is progressively increased on the same oxide, forms an ideal system for investigating the properties as the electrodes are made superconducting. The I-V characteristics for the first four of these junctions are shown in Fig. 17. The remaining junctions were too resistive to be reliably measured in our experimental arrangement. When no a-Ge is present the characteristic is typical of MOM junctions with both electrodes superconducting and $T \lesssim T_c$.[24] The temperature is determined from the BCS energy gap values for Al.[25] With 15-Å a-Ge present the I-V characteristic is typical of that for electrodes having different transition temperatures.[26] The knee at low voltage gives the energy-gap difference, $\Delta_2 - \Delta_1 = 28\ \mu$V at 1.16 K. As the a-Ge thickness is increased to 23 Å the curve remains the same except that the knee is more rounded and the jump at $\Delta_2 + \Delta_1$ is not as sharp. With 35-Å a-Ge present in the junction the characteristics are quite different—the features of ordinary superconductive tunneling are no longer present. Instead, there is a much straighter curve with two slight bends: a bend upward at 115 μV and a decrease in slope at approximately 260 μV. The slope at zero bias has also altered considerably.

Since $T/T_c = 0.93$ in these measurements, any small change in T_c and Δ is made especially noticeable. The energy-gap difference for the junctions with 15-Å and 23-Å a-Ge could arise from an alloying of the Al counterelectrode with Ge. Alloying Ge into Al is known to result in a substantial increase in T_c.[27] Alternatively, the internal stress of the evaporated a-Ge film[28] may cause a strain-induced enhancement of T_c in Al.[29] However, this enhancement should scale with a-Ge thickness, in contrast to the same increase for both 15-Å and 35-Å a-Ge. Recently there has been an attempt[30] to explain the enhancement of T_c in Al-Ge mixtures by invoking excitonic superconductivity.[31] This problem has not yet been resolved.

Additional information is obtained from the tunnel junctions using Sn as counterelectrode, as shown in Fig. 16. Sn was chosen because its transition temperature, $T_c = 3.7$ K, is greater than that of Al. The I-V characteristics for the first four Al-Al_2O_3-Ge-Sn junctions are shown in Fig. 18, where the measuring temperature is 1.3 K, just above the 1.25 K transition temperature for Al. These curves are all similar to each other and are typical of junctions with one superconducting electrode well below its transition temperature.[26] Some structure is present at about 0.8 mV, especially noticable in the junction with 23 Å a-Ge. This may be caused by the edge effect, in which thin sections of the Sn electrode at the edge of the strip have an increased T_c. No edge protection was provided for these junctions. Figure 19 shows the same junctions measured at 1.16 K, below but near T_c for the Al electrode. The curves for 0-Å and 15-Å a-Ge are what is expected for junctions with two superconducting electrodes differing greatly in T_c.[26] The flat portion of the curve is the jump across the

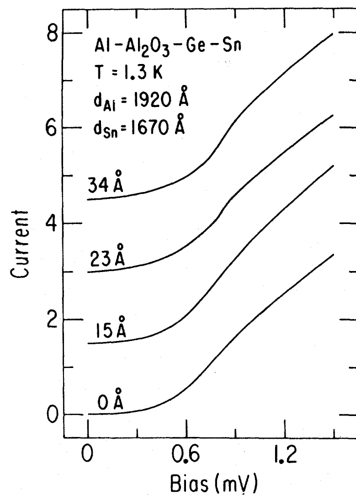

FIG. 18. Current as a function of voltage at 1.30 K for Al-Al_2O_3-Ge-Sn tunnel junctions. The current scales per division for the different a-Ge thicknesses are (a) 0 Å: 1.67×10^{-8} A; (b) 15 Å: 5×10^{-8} A; (c) 23 Å: 3.33×10^{-9} A; and (d) 34 Å: 3.33×10^{-10} A. Current axis is offset for clarity.

negative resistive region. The exact place for the jump depends on such parameters as direction and rate of voltage sweep. With 23-Å a-Ge in the junction the discontinuity has disappeared and the rise is more gradual, forming two steps. With 34-Å a-Ge the rise is even more gradual and the second step has disappeared. The onset of the change now begins approximately 40 μV lower in bias voltage than in the other curves. No change in Δ is observable in Figs. 18 and 19. Since $T/T_c = 0.34$ it would take fairly strong change to be visible in these curves. The fact that the energy gap in the superconducting Sn is present and not altered by up to 34-Å a-Ge demonstrates that tunneling is the dominant conduction mode across the oxide for these junctions. For a-Ge thickness up to at least 34 Å direct tunneling from metal electrode to metal electrode is taking place.

In Fig. 19 it is evident that the negative resistance region has disappeared for 23- and 34-Å a-Ge. It would be attractive to interpret the deviations from ordinary superconductive tunneling in both sets of junctions as arising from gapless superconductivity induced in the Al by the presence of a-Ge in the junction. There are, however, alternative explanations for this behavior. For instance, the loss of the negative resistance region may be an artifact of the measuring circuit. A more thorough experimental investigation is needed before a clear interpretation can be made.

VII. TUNNEL-JUNCTION CAPACITANCE

In this section we will treat the tunnel junctions as capacitors and see what can be learned about the density of states in the a-Ge from a study of sample capacitance. The most important and obvious capacitance is that of the oxide, C_{ox}. When a potential is applied across the oxide, charge accumulates on each side. In the semiconductor, because of a finite density of states, the charge is not at the oxide-semiconductor interface, but is distributed into the bulk of the semiconductor with a characteristic distance given by the screening length. This space-charge region exists in the semiconductor even with no applied bias and arises from the equilibration of the Fermi levels in the metal and semiconductor. Because the added charge is distributed in the space-charge layer the measured capacitance should be smaller than the geometrical capacitance of the oxide. This is equivalent to a space-charge capacitance C_{sc} in series with C_{ox}. A comparison of MOM and MOSM junctions formed with the same oxide shows no difference in capacitance at 300 K to within experimental error, independent of a-Ge thickness. There was no change in capacitance with measuring frequencies from 300 to 10 Hz, and the capacitance was independent of bias up to ±1 V to within 1%. From the experimental error a lower limit can be placed on C_{sc}. For a 30-Å oxide, $C_{sc} \geq 20\, C_{ox}$. This means that the electrons are accumulating within 4 Å of the oxide. The a-Ge is behaving like a metal.

A simple extension of the model of the junction capacitance gives a more reasonable explanation for a lack of change in capacitance at 300 K. If the effects of surface states are included the equivalent circuit is as shown in Fig. 20. R_s and C_s of the

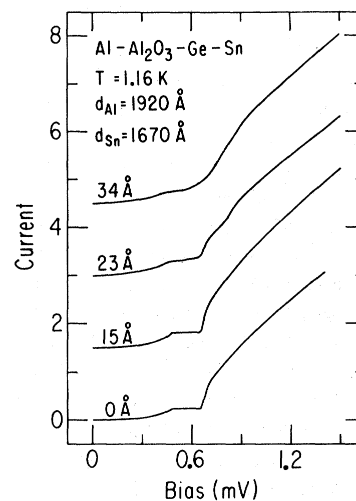

FIG. 19. Current as a function of voltage at 1.16 K for Al-Al_2O_3-Ge-Sn tunnel junctions. The current scales per division for the different a-Ge thicknesses are (a) 0 Å: 1.67×10^{-8} A; (b) 15 Å: 5×10^{-8} A; (c) 23 Å: 3.33×10^{-9} A; and (d) 34 Å: 3.33×10^{-10} A. Current axis is offset for clarity.

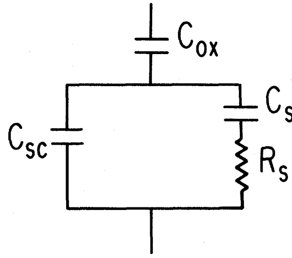

FIG. 20. Equivalent circuit for tunnel junction capacitance including oxide (C_{ox}), space-charge (C_{sc}), and surface states (R_s and C_s).

surface states arise because of the time constant associated with surface traps. The parallel branches arise because charge is added simultaneously to the space-charge region and to the surface states. The equivalent parallel capacitance for the surface is

$$C_P = \frac{C_s + C_{sc}(1+\omega^2\tau^2)}{1+\omega^2\tau^2} , \tag{10}$$

where $\tau = R_s C_s$. Since there was no measured frequency dependence of capacitance, we shall take the low-frequency limit. The failure to detect a difference in MOM and MOSM capacitances will now be attributed to C_s. Assuming a continuous energy-independent density of surface states N_s, the increase in charge occupying surface states can be written as a product of N_s, the area, electronic charge, and the change in energy

$$\Delta Q = A N_s e \Delta e V \ . \tag{11}$$

A derivative can be taken to obtain an expression relating N_s to C_s,

$$N_s = C_s / e^2 A \ . \tag{12}$$

Using the limit of detectability of change in capacitance, $N_s \geq 2.5\times10^{14}\ \mathrm{eV^{-1}\ cm^{-2}}$. The failure to see C_{sc} in the MOSM system can thus be explained by a very high density of surface states, on the order of one per surface atom in the oxide-semiconductor (O-S) interface region. A large surface state density does more than mask the space-charge capacitance; it greatly reduces the potential drop across the space-charge region and makes it difficult to change the magnitude of this potential drop.

As the temperature is decreased the MOSM capacitance does change and becomes frequency dependent. This is expected and is easily explained by including the a-Ge bulk capacitance (C_{Ge}) and resistance (R_{Ge}). The oxide and the a-Ge layer form two parallel RC combinations in series with each other. The measured parallel capacitance C_P is

$$C_P = \frac{C_{ox} C_{Ge}}{C_{ox} + C_{Ge}} \quad \text{as } \omega \to \infty \tag{13}$$

and

$$C_P = \frac{R_{ox}^2 C_{ox} + R_{Ge}^2 C_{Ge}}{(R_{ox} + R_{Ge})^2} \quad \text{as } \omega \to 0 \ , \tag{14}$$

where R_{ox} is the oxide resistance and ω is the measuring frequency. The low-temperature frequency dependence arises from the transition from one domain to the other. At room temperature R_{Ge} is so small that the $\omega \to 0$ limit prevails over the entire measured frequency range and $C_P = C_{ox}$. A detailed study of low-temperature capacitance was not undertaken.

VIII. DISCUSSION

It is concluded from this investigation of electron tunneling into a-Ge that the low-temperature conductance is dominated by the a-Ge high-field conductivity. This necessitates a simple correction to obtain the conductance determined by the junction interface region independent of the bulk a-Ge properties. This correction works well for junctions with thick a-Ge layers where the correction parameters can be experimentally determined. With thin films of a-Ge the high-field conductivity blends smoothly with the junction conductance, making extraction of the junction conductance impossible without a prior knowledge of both tunneling and conductivity mechanisms. For junctions with sufficiently thin a-Ge thickness, $t \simeq 100$ Å, the correction to the G-V characteristics for the a-Ge conductance is negligable away from zero bias.

An exponential drop in conductance with increasing a-Ge thickness is observed for very thin a-Ge layers. This is explained by considering incomplete surface coverage of a-Ge. A consequence of this is that an upper limit can be placed on the distance the electrons tunnel into the bulk of the a-Ge, varying from 28 Å at 300 K to 50 Å at 4.2 K. The incomplete-surface-coverage interpretation requires tunneling probability to be determined by the O-S interface, including only the first few monolayers. A study of junction capacitance strongly supports this. The absence of a change in capacitance of the tunnel junction structures due to the presence of a-Ge leads to the conclusion that there is a high density of surface states at the oxide-semiconductor interface.

The temperature dependence of zero-bias conductivity for tunnel junctions with thick a-Ge layers is well described by the $\ln G$ vs $T^{-1/4}$ behavior of the variable-range tunneling model down to temperatures where bulk a-Ge effects become noticable. Comparison of Eqs. (3) and (7) show that it is anticipated that $T_1 \simeq 2T_0$. However, the data for a-Ge show that $T_1 \simeq 0.04\,T_0$. The only system that comes close to behaving as expected is room-temperature-deposited a-Si, for which $T_1 \simeq T_0$.[3,9] This discrepancy can be explained within the variable-

range model by attributing different values to α and $N(E)$ in the expressions for T_0 and T_1. The α value used in T_0 is that for states in the gap at the Fermi energy. Band bending near the O-S interface in the tunnel junction will move the band edges nearer to E_F, resulting in a smaller α_s and causing T_1 to become smaller. The band bending or a higher degree of disorder near the interface may cause $N(E)$ to be greater in T_1 than in T_0, also decreasing T_1. The upper limits placed on the possible tunneling range for a-Ge by the partial surface-coverage data necessitate modifications of Eqs. (2) and (3). The derivation[9] assumes that the tunneling range into the a-Ge is much greater than the oxide thickness, while experiment indicates they are of comparable magnitude. However, to first order, a modification yields an increase in the numerical coefficient for T_1 over the value in Eq. (3).

The variable-range tunneling model fails to account for the minimum at zero bias other than by requiring the density of states minimum to lie at the Fermi level. This objection may be dealt with by including indirect tunneling processes away from zero bias. Only at zero bias would direct tunneling take place and there would be a rapid increase in phonon-assisted hopping in the a-Ge as electrons tunnel to and from states further away from E_F. Also, α_s decreases in tunneling to states closer to the band edges. We have seen that the capacitive measurements indicate a high density of surface states at the O-S interface. The temperature dependence of the conductance at zero bias may still involve variable-range tunneling in the presence of these states.

The question of whether or not electron tunneling yields information about the density of gap states in a-Ge can now be discussed. The limits on the possible tunneling range make it impossible to obtain information about the bulk a-Ge properties. At most tunneling tells us something about the interface region, including only the first few layers of a-Ge. In order to avoid having the Fermi level lie at the density of states minimum it is necessary to invoke indirect processes away from zero bias, thereby restricting density of states information to the Fermi level. Finally, since the variable-range tunneling model assumes long tunneling ranges, it would require modification before attempting to ascribe meaning to a density of states derived even for zero bias.

The discussion so far has assumed that the tunnel-junction conductance is indeed tunneling conductance rather than another mechanism. This can only be demonstrated by the observation of superconductive tunneling. Since these junctions become highly resistive at low temperatures, superconductive tunneling is observed only for junctions with a-Ge thicknesses $t \lesssim 35$ Å. In such cases the tunneling is through metallic shorts in the a-Ge layer. At higher biases, since MOM tunneling is relatively bias independent, the MOSM conductance is thus by tunneling. For all junctions tunneling is undoubtedly the dominant mechanism at high temperatures for all biases and at high biases for all temperatures. For junctions with complete a-Ge surface coverage other mechanisms may become competitive as the total conductance decreases at sufficiently low biases and temperatures. The question is not so much whether or not tunneling is taking place at low biases and temperatures, but rather why is it being frozen out. Furthermore it is the a-Ge in only the first few monolayers that is freezing out the tunneling.

It is appropriate to point out the striking similarity of the G-V curves for tunneling into amorphous semiconductors with the curves for the giant resistance anomaly,[32,33] which arises in tunneling through barriers formed using oxides of transition metals. Both systems have conductances symmetric about a minimum at zero bias, the conductance increasing several orders in magnitude as the bias is increased to ± 1 V. Since the giant resistance anomalies so far found and investigated have involved magnetic oxides, Gupta[34] attempted to explain the anomaly by using scattering from a concentrated system of paramagnetic impurities. He found antiferromagnetic coupling of the impurity spins for a sufficiently dense system. However, the calculated effect on tunneling fails to obtain a large enough change in conductance. Nielsen[33] proposed that his oxides formed narrow-band-gap amorphous semiconductors and that electrons tunnel into the amorphous semiconductor. However, the increase in thickness of the barrier with the addition of the transition-metal oxide is too small to account for the magnitude of the change in zero bias conductance for several cases.

Giaever and Zeller[35,36] have proposed that the resistance anomaly may be caused by the inclusion of small metallic particles in the oxide. Several of the observed anomalies seem to be well described by the model, but others, such as those involving TiO_2,[33] require an extrapolation of the model to the limit of very small particles. The physical basis for the model is that the metal particle can only accept electrons in increments of unit charge. This creates a finite energy difference between the highest occupied energy level and the lowest unoccupied level. On applying a bias to the tunnel junctions, electrons can only tunnel through longer alternate paths until sufficient energy is attained to reach the lowest unoccupied level. As the particle size decreases the level spacing increases and the effect becomes more pronounced. This model works well when dealing with well-defined metallic particles of fairly uniform size. The problem arises

in taking the limit in decreasing the particle size. In this limit the well-defined electron states go over to a distribution of localized impurity states and the model reduces to a density of states model. There is no longer a clear reason why a symmetric conductance minimum should lie at zero bias, and the model suffers from the same defects of any direct density of states interpretation.

The similarity of the tunneling into a-Ge and the giant resistance anomaly is not just in the appearance of the G-V characteristics. The large concentration of surface states at the oxide-semiconductor interface may be the analog of the spin states found in transition-metal oxides. A surface effect is consistent with the interpretation of tunneling into very thin a-Ge layers as showing surface coverage. We feel that a model explaining one system should be able to explain in the other.

ACKNOWLEDGMENTS

I am indebted to H. Fritzsche for suggesting this problem and for encouragement and guidance throughout the investigation.

---

*Research supported by the Air Force Office of Scientific Research, Office of Aerospace Research, USAF, under Contract No. F44620-71-C-0025. We have also benefited from support of the Materials Research Laboratory of the National Science Foundation.

†Submitted in partial fulfillment of the requirements for the Ph.D. degree of The University of Chicago.

‡Present address: Dept. of Physics, Oregon State University, Corvallis, Ore. 97330.

[1]J. W. Osmun and H. Fritzsche, Appl. Phys. Lett. 16, 87 (1970).
[2]C. W. Smith and A. H. Clark, Thin Solid Films 9, 207 (1972).
[3]J. J. Hauser, Phys. Rev. B 8, 2544 (1974).
[4]J. A. Sauvage and C. J. Mogab, J. Non-Cryst. Solids 8–10, 607 (1972).
[5]C. Konak and J. Stuke, Phys. Status Solidi A 9, 333 (1972).
[6]W. A. Harrison, Phys. Rev. 123, 85 (1961).
[7]N. F. Mott, Philos. Mag. 13, 989 (1966).
[8]M. H. Cohen, H. Fritzsche, and S. R. Ovshinsky, Phys. Rev. Lett. 22, 1065 (1969).
[9]J. A. Sauvage, C. J. Mogab, and D. Adler, Philos. Mag. 25, 1305 (1972).
[10]N. F. Mott, Philos. Mag. 19, 835 (1969).
[11]J. W. Osmun, Solid State Commun. 13, 1035 (1973).
[12]W. E. Spear and P. G. LeComber, J. Non-Cryst. Solids 8–10, 727 (1972).
[13]J. W. Osmun and H. Fritzsche, AIP Conf. Proc. 20, 333 (1974).
[14]W. F. Brinkman, R. C. Dynes, and J. M. Rowell, J. Appl. Phys. 41, 1915 (1970).
[15]N. Croitoru and L. Vescan, Thin Solid Films 3, 269 (1969).
[16]M. Morgan and P. A. Walley, Philos. Mag. 23, 661 (1971).
[17]V. Ambegoakar, B. I. Halperin, and J. S. Langer, Phys. Rev. B 4, 2612 (1971).
[18]J. J. Hauser and A. Staudinger, Phys. Rev. B 8, 607 (1973).
[19]H. Fritzsche, J. Non-Cryst. Solids 6, 49 (1971).
[20]K. E. Gray, Solid State Commun. 13, 1787 (1973).
[21]D. Henderson (unpublished).
[22]T. M. Donovan and K. Heinemann, Phys. Rev. Lett. 27, 1794 (1971).
[23]A. Barna, P. B. Barna, and J. F. Pocza, J. Non-Cryst. Solids 8–10, 36 (1972).
[24]I. Giaever and M. Megerle, Phys. Rev. 122, 1101 (1961).
[25]B. L. Blackford and R. H. March, Can. J. Phys. 46, 141 (1968).
[26]I. Giaever, H. Hart, and K. Megerle, Phys. Rev. 126, 941 (1962).
[27]J. J. Hauser, Phys. Rev. B 3, 1611 (1971).
[28]M. A. Paesler, in *Proceedings of the Fifth International Conference on Amorphous and Liquid Semiconductors, Garmisch-Partenkirchen* (Tayler & Francis, London, 1974) p. 229.
[29]H. A. Notarys, Appl. Phys. Lett. 4, 79 (1964).
[30]C. C. Tsuei and W. L. Johnson, Phys. Rev. B 9, 4742 (1974).
[31]D. Allender, J. Bray, and J. Bardeen, Phys. Rev. B 7, 1020 (1973).
[32]L. Y. L. Shen and J. M. Rowell, Phys. Rev. 165, 566 (1968).
[33]P. Nielsen, Phys. Rev. B 2, 3819 (1970).
[34]H. M. Gupta, J. Phys. C 6, 686 (1973).
[35]I. Giaever and H. R. Zeller, Phys. Rev. Lett. 20, 1504 (1968).
[36]H. R. Zeller and I. Giaever, Phys. Rev. 181, 789 (1969).